THE EFFECTS OF THE TIP CLEARANCE ON THE PERFORMANCE OF SMALL-SCALE TURBOPUMPS FOR ORC APPLICATIONS; ANALYSIS AND MODELING

Sajjad Zakeralhoseini*

Laboratory for Applied Mechanical Design
Institute of Mechanical Engineering
École Polytechnique Fédérale de Lausanne
Neuchâtel, Switzerland
sajjad.zakeralhoseini@epfl.ch

Jürg Schiffmann

Laboratory for Applied Mechanical Design
Institute of Mechanical Engineering
École Polytechnique Fédérale de Lausanne
Neuchâtel, Switzerland
jurg.schiffmann@epfl.ch

*Corresponding Author

ABSTRACT

In this paper, the influence of tip clearance on the performance of small-scale turbopumps is studied numerically on extensive parameter ranges suitable for organic Rankine cycle applications. A novel and fully parameterized design model is developed and used to generate a wide range of turbopumps and their fluid domains to carry out three-dimensional computations across the impeller stage. Impellers are investigated at different operating conditions and the accomplished results are analyzed to characterize the performance at design and off-design conditions. The CFD calculations demonstrate that the slip factor is dependent not only on its geometrical parameters as considered by most correlations but also on its operating conditions. The slip factor decreased almost linearly as the flow rate increased. In addition, the tip clearance ratio influences the slip factor and its influence is non-linear. The head rise decreases as the tip clearance ratios increased, however, for radial impellers, the higher head rise was observed for small tip clearance ratios (<0.10). The results are employed to infer reduced-order models for considering the tip clearance effect in the early-phase design process of small-scale turbopumps. The models predicted the CFD data with the average relative deviation of 3.6 and 5.8 for the slip factor and the head loss coefficient, respectively.

Keywords: ORC, Turbopumps, CFD, Slip factor, Head rise, 1D modeling

1. INTRODUCTION

General theories and design approaches for conventional large-scale pumps are well-established and the technology is well-matured. However, emerging applications such as Organic Rankine Cycle (ORC) systems for waste heat recovery require a combination of low-rated flow and high-pressure rise with smaller geometrical dimensions. Although reduced-order models predict the performance of geometrically similar pumps as a function of specific speed and the Reynolds number, a turbopump's performance is also affected by various additional parameters, which amplify in geometrical down-scaling such as higher values of relative roughness and tip clearance. The tip clearance is recognized to have mostly adverse effects on the performance of centrifugal machines and it is, therefore, necessary to predict its influence correctly in the design process of a turbopump.

In an early study, Wood *et al.* (1965) reported that unshrouded impellers of centrifugal pumps performed better in terms of cavitation in comparison to shrouded impellers. Their observations suggest that at best efficiency, the slip increases and the head coefficient decreases with increasing tip clearance and for very small relative tip clearances, higher efficiency can be expected for unshrouded impellers. Pampreen (1973b) studied scaling effects on the performance of axial fans and centrifugal compressors. His results suggested that Reynolds stresses outweigh the viscous stress and the compressor efficiency is more influenced by the tip clearance than the Reynolds number. Senoo and Ishida (1984) proposed an estimation method to predict the performance of unshrouded centrifugal impellers at design and off-design conditions. The method was compared with experimental data of different centrifugal compressors and the results suggest that the influence of tip clearance on the efficiency deterioration gets smaller as the flow rate is reduced. In another

study, Ishida *et al.* (1989) experimentally investigated the secondary flow pattern at the outlet of an unshrouded radial and a backswept impeller. They suggest that the secondary flow induced by the tip clearance is due to the shear stress component, which is normal to the blade surface and acts against the adverse pressure gradient. The observation suggested that the relative flow angle is hardly affected by the tip clearance at the outlet of the radial impeller, while it is reduced significantly with increasing the tip clearance in the case of the backswept impeller, therefore suggesting an increased effect on the slip factor. Recent work by Diehl *et al.* (2020) on small-scale centrifugal compressors showed that the loss induced by the tip clearance is independent of the Reynolds number.

Based on three-dimensional Computational Fluid Dynamics (CFD) simulations, Aknouche (2003a) developed a model to predict the performance deterioration due to the tip clearance of turbopumps. The model accounts for the tip clearance losses induced by mixing the tip leakage flow with the main flow and the increased blockage caused by the lower streamwise velocity of the leakage flow compared to the main flow. Through a numerical study, Eum and Kang (2004) computed and analyzed the loss distribution of a centrifugal compressor at different tip clearances. Based on the results, they identified the suction-shroud corner as the region where possibly the highest loss due to the tip clearance occurs and proposed a simple correlation for predicting the specific work reduction due to tip clearance leakage.

Since the reduced-order models available in the literature are developed for large-scale turbopumps, the influence of geometric down-scaling is not addressed. Thus, they might lead to impractical or even infeasible designs far from optimum for small-scale applications. Therefore, whether the adoption of such models and tools is still applicable at the small-scale is a matter of argument, especially when design parameters like the relative tip clearance, which is one of the most distinct differences between large-scale and small-scale strongly affect the flow structure inside such machines.

This paper summarizes the results on the influence of tip clearance on the performance of small-scale turbopumps based on a numerical approach. The variations of the slip factor and the head rise caused by the tip clearance are estimated as a function of influential parameters, providing necessary models for considering the tip clearance effect in the early-phase design process of small-scale turbopumps.

2. METHODOLOGY

Parametric impeller design. As highlighted in the previous section, three-dimensional viscous computations are necessary to obtain a turbopump geometry with acceptable efficiency levels and suitable for small-scale applications. To develop new reduced-order models with regards to slip and tip clearance losses for the accurate performance prediction of small-scale centrifugal pumps, Neural Network (NN) models fed with CFD data are employed in this work. To build a robust model, a large number of diverse training data is required. Therefore, a parametric blade design model is developed and used to generate an extensive range of turbopump geometries for their assessment with a CFD-based approach. The methodology implemented for this work is summarized in Figure 1.

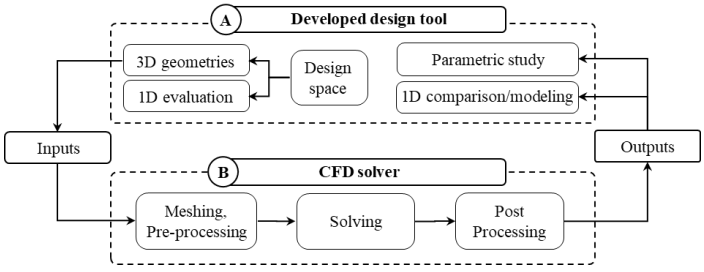

Figure 1 – Methodology flowchart

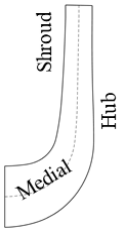

Figure 2 – Meridional profile generated with the developed method

For given main dimensions of a turbopump, the meridional profiles of hub and shroud are necessary to generate the full blade shape. The approach adopted in this study is based on a combination of methods proposed by Zou *et al.* (2012) and Le *et al.* (2017). The advantage of the developed approach is that the

meridional shape, which has a dominant effect on flow patterns and performance is built systematically, i.e. for a chosen area or velocity distribution from the impeller eye to its outlet, which makes it very suitable for fast automated generation of different geometries. The medial axis as depicted in Figure 2 is the first profile that is generated based on the statistical model developed by Zou *et al.* (2012). The hub and shroud profiles are then obtained through the medial axis theory presented in Lu *et al.* (2017). The mathematical equations of blade cambers are obtained through the Stepanoff method (1957). The thickness and shape functions are introduced to complete the blade shaping based on considerations suggested in Gülich (2010). To achieve the highest suction performance, the blade is shaped 3D at the LE with an elliptic profile and it has been converted to 2D at the trailing edge (TE) for easier manufacturing (see Figure 3).

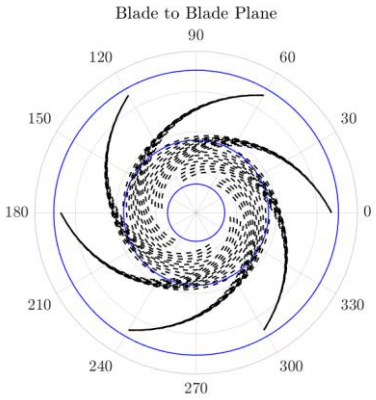

Figure 3 – The camberline profiles

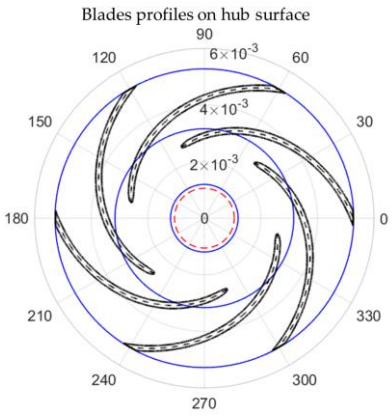

Figure 4 – Hub blade section

Numerical scheme. The parametric blade design tool is employed to generate turbopump geometries within the parametric ranges listed in Table 1 using a factorial design approach, leading to 72 shrouded and 504 unshrouded to be assessed with CFD. The diversity of the analyzed turbopump geometries is illustrated in Figure 5. The angle definition is shown in Figure 6 and the clearance gaps are normalized based on the blade outlet width. The parameters are selected based on the requirements of ORC systems for waste heat recovery applications (Rosset *et al.*, 2021, 2018b). The scaling is based on Buckingham's Pi-theorem and the fluid is R245fa with density and dynamic viscosity of 1311.9 kg.m^{-3} and 3.525 ×10^{-4} Pa.s respectively at the inlet conditions.

Table 1 – Parametric ranges of ORC turbopumps

Outlet diameter	13, 16, 18, 24	(mm)
Blade angle	15, 22.5, 27.5, 32, 50, 90	(°)
No. blades	5, 6, 7	(-)
Tip clearance ratio	0.05, 0.1, 0.15, 0.2, 0.3, 0.4, 0.6	(-)
Rotational speed	40, 50, 63.5, 75	(krpm)
Reynolds number	1.2×10^6 – 2.3×10^6	(-)

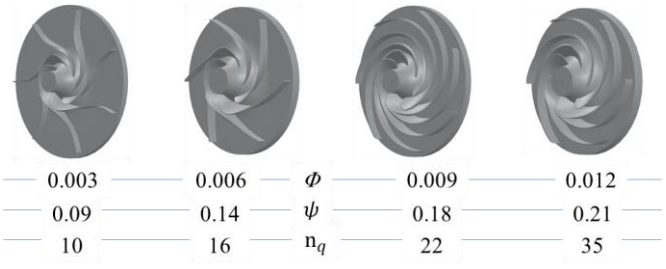

Figure 5 – The diversity of studying turbopumps (values are post-computed)

To assess and analyze the performance and detailed flow patterns of the different turbopumps, the geometries are sent to CFD. The computational domain consists of an inlet duct and the impeller. The inlet duct length is 10 times the impeller diameter and is meshed with a hexahedral structured grid with an expansion ratio of 1.8. A structured mesh is adopted for the impeller and its size varies between 800,000 to 1,500,000 elements. The sizing is based on initial manual evaluation and mesh independence in extreme ranges of parameters. Boundary layer treatments and near-wall elements are controlled based on y^+ evaluation to ensure its values lie in the range of the turbulence model validity (Mentor (2003b)). The clearance layers are higher than 45 with an end ratio of 30 to 43.

At inlet and outlet, the total inlet pressure and the mass flow rate are set respectively. The walls are treated with no-slip and rough conditions. The turbulence is modeled with Mentor's shear stress transport model (2003b) due to its capability in the prediction of separation and secondary flows in rotary domains. The rough wall condition moves the logarithmic velocity profile closer to the wall and influences the efficiency, especially in small-scale applications, therefore its influence is accounted for in the near-wall treatment of the turbulence model. The time-averaged equations of mass and momentum assuming steady-state condition and incompressible flow are solved numerically with the CFX solver. Though head rise, efficiency, and flow conditions at the outlet, which are of interest to this research are converged after a small number of iterations i.e. 150, a minimum number of iterations of 400, and RMS residual target of 10^{-5} are set for the convergence criteria. The developed tools shown in Figure 1 propagates the problem to six workstations running on Intel Xeon Processor E5-1650 v3 3.50 GHz.

3. RESULTS AND DISCUSSION

The results obtained from the numerical approach enable the identification of fundamental variables, such as slip factor, efficiency, head coefficient, and head loss due to the tip clearance.

3-1. Slip factor

Prior work highlight that the outflow at the tip (trailing edge) is not blade-congruent and deviates from the path imposed by blade shape due to the non-uniform velocity profiles and the Coriolis acceleration (Wiesner, 1967). Thus, it leaves the impeller with the flow angle β_2 that is smaller than the metal blade angle β_{2B}. This "slip" decreases the circumferential component of absolute velocity by ΔC_{u2} compared to the ideal case, and therefore changes the velocity triangle at impeller outlet as depicted in Figure 6.

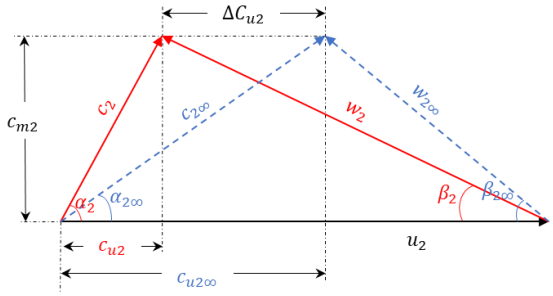

Figure 6 - Velocity triangle at the impeller outlet

The slip factor is defined to consider flow deviation effects to decrease the energy transmission to the fluid. In this paper the slip factor is defined in Eq. (1) and by using the velocity triangle at the impeller outlet:

$$\gamma = 1 - \frac{c_{u2\infty} - c_{u2}}{u_2} \tag{1}$$

where $c_{u2\infty}$ is the circumferential component of absolute velocity for an impeller with an infinite number of blades. Due to the significant impact of the slip factor on the performance of centrifugal impellers, it has been studied by several researchers. However, no model has yet been found to predict slip factors in general. The most accepted correlations are employed for comparison in the following section for shrouded and unshrouded impellers.

Shrouded impeller. In Figure 7, the relative deviation ($[X_{predicted,i}-X_{CFD,i}]/ X_{CFD,i}\times100$) of slip factors predicted by correlations are compared with the corresponding values calculated based on CFD for all shrouded impellers. Relative (e_i) and mean relative errors ($\bar{e}$) as well as standard deviation (σ) are considered for evaluation of predicting correlations. As the plots suggest, the Von Backström (2006) correlation provides the best agreement with CFD results, predicting 100% of the values within a relative deviation of ±10%. His correlation unified several validated slip factor models. The correlation of Wiesner (1967) is the second most accurate method with 90.1% of the CFD results within a relative deviation of ±10%. The comparison with correlations of Stodola (1927) and Stanitz (1952) shows that only 2% and 60%

of CFD data are predicted within ±10% relative deviation respectively, which is not satisfactory. The very good agreement of CFD results of shrouded-impeller with the well-known correlations of Von Backström (2006) and Wiesner (1967) validates the methodology and accuracy of CFD results as the mean relative difference and standard deviation calculated to be 2.1% and 1.75% respectively for Von Backström's (2006) correlation.

To illustrate the trend of data, the slip factors computed based on CFD are compared with Von Backström (2006) correlation in Figure 8. The data suggest that at a constant number of blades, the slip factor initially decreases and then increases with increasing blade angle β_{2B}, leading to the lowest slip factor at β_{2B} of 50°; a trend, which is not observed with the Von Backström (2006) correlation. Contours and vectors of normalized relative velocity (w/u_2) around the blades are shown in Figure 9. The figure suggests vortices causing severe flow deviation at the TE that grow with increasing β_{2B} and are suggested to increase the slip factor with β_{2B}.

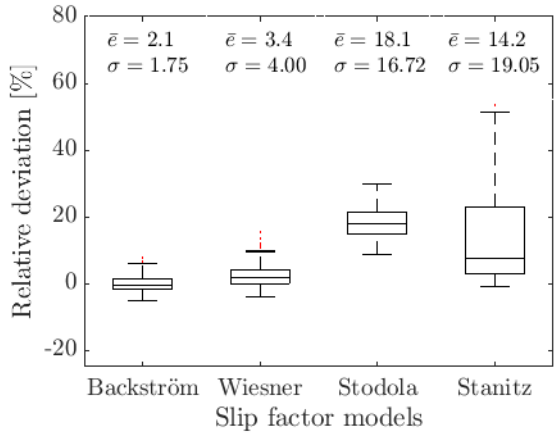

Figure 7 – Relative deviation of slip factors predicted with correlations from CFD (shrouded impellers)

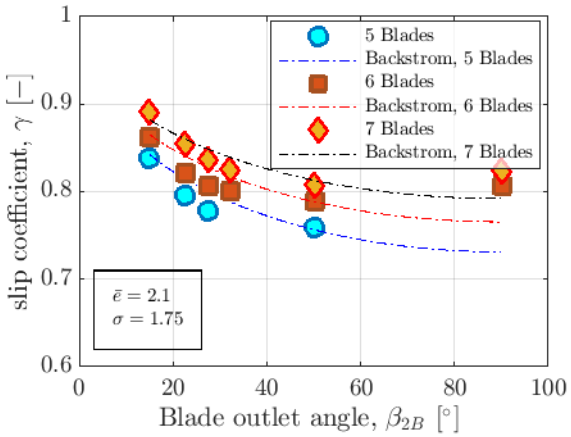

Figure 8 – Change of slip factors with blade outlet angle and number of blades (shrouded impellers)

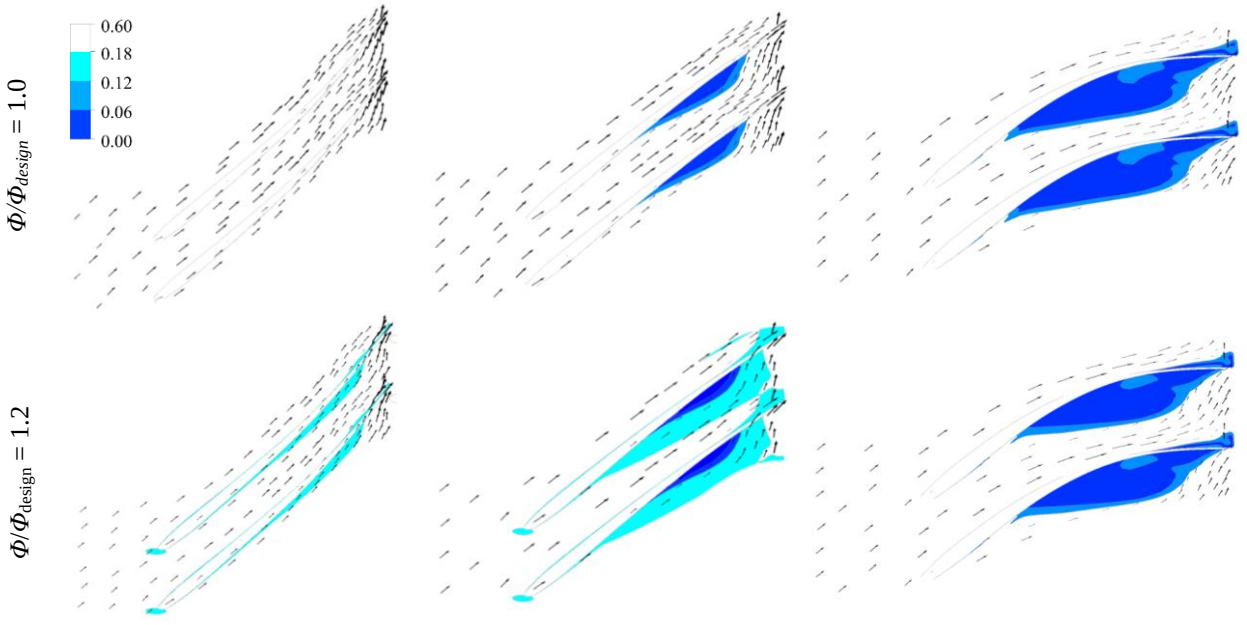

Figure 9 – Contours and vectors of normalized velocity (w/u_2) at mid-span for shrouded impellers

Unshrouded Impellers. Figure 10 presents the slip factors of unshrouded impellers based on CFD results for different β_{2B} and for varying relative tip clearance for impellers designed at 50,000 rpm operating at

their design flow rate. For each design, the corresponding value of the shrouded impeller is represented with a blue circle. While the slip factor values vary significantly with tip clearance, they follow almost the same trend as shrouded impellers, namely decreasing and then increasing with β_{2B}.

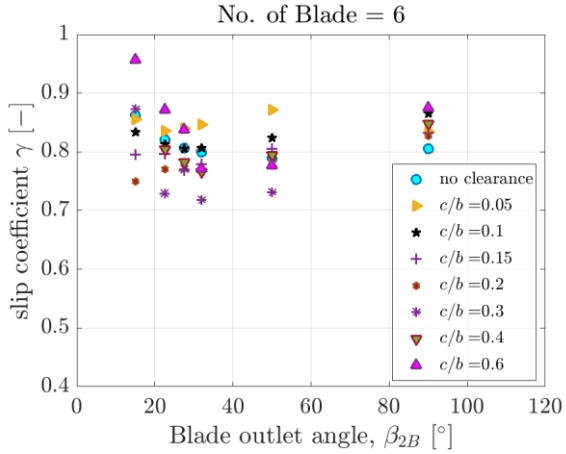

Figure 10 – Change of slip factors with tip clearance and blade outlet angle at different numbers of blades

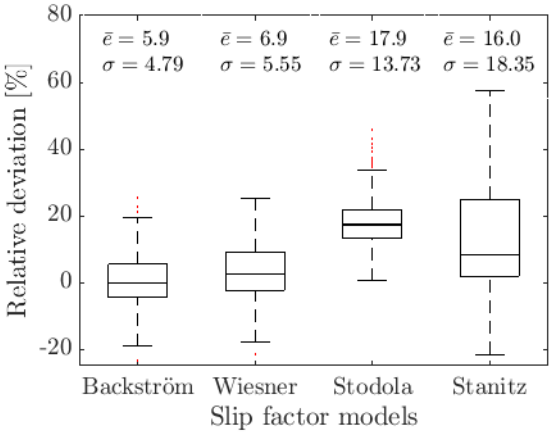

Figure 11 – Relative deviation of slip factors predicted with correlations from CFD results for all impellers

It is expected that a higher deviation from CFD results would be observed when correlations are applied to unshrouded impellers. Such comparison is represented in Figure 11. According to the results, slip factors computed from CFD results deviate by ±20% compared to Von Backström's (2006) and Wiesner's (1967) correlations. The relative deviation is much higher for Stodola (1927) and Stanitz (1952). The reason for such deviation is explained in the following.

In Figure 12 (a), the slip factors are plotted against β_{2B} for shrouded and selected unshrouded impellers for various mass-flows, suggesting that the slip factor is less dependent on the flow rate at a larger blade outlet. Referring to Figure 9, at a larger β_{2B}, the core flow is influenced more profoundly by secondary flows, even at the design point. Therefore, additional flow disturbance induced by off-design operation seems to have a lower influence on velocity components at the TE and therefore the slip factor is less influenced by the flow rate. Figure 12 (b) suggests the slip factor decreases as the flow coefficient increases for both shrouded and unshrouded impellers. This decrement, however, varies between shrouded and unshrouded impellers with a more pronounced effect for unshrouded impellers (represented by squares in the figure).

The slip factors are plotted against tip clearance ratios for design mass flow operation in Figure 12 (c). The 0-value on the x-axis corresponds to shrouded impellers. The results indicate that the variation of slip factors against tip clearance ratios is not linear and increases for small ratios of tip clearance (<0.10) and then decreases to reach minimum values at intermediate tip clearance ratios before rising again for very large tip clearances. The tip leakage flow driven by the pressure difference between the pressure and suction side of the blade enters the core passage flow with a different streamwise velocity component. The consequent mixing results in the generation of vortices within the core flow passage and thereby change velocity components and the velocity triangle significantly as demonstrated in the literature (2003a). Concisely, the slip factor decreases with increasing β_{2B} and flow rate and it rises with the increasing number of blades. It increases at small tip clearance ratios and then it falls to reach a minimum value at a moderate tip clearance.

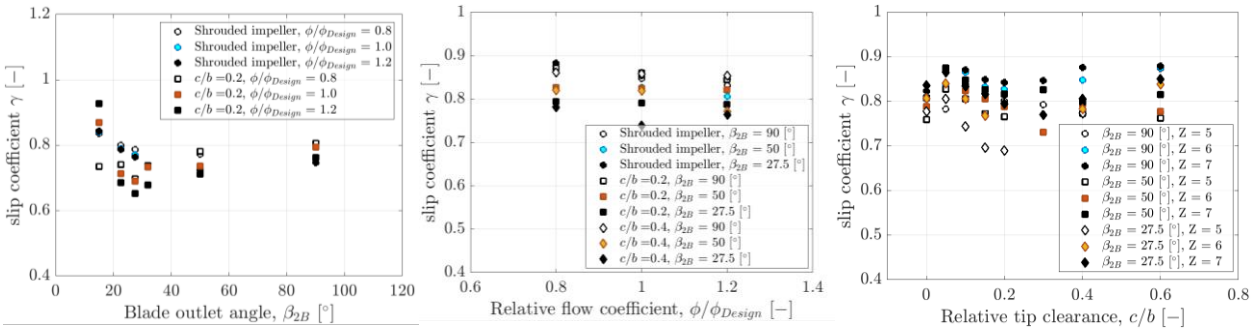

(a) (b) (c)

Figure 12 – Effects of blade outlet angle (a), flow rate (b), and tip clearance ratios (c) on the slip factor

3-2. Performance reduction due to the tip clearance

Tip clearance reduces the impeller Euler head, thus the tip clearance influences the impeller head rise through both the reduction of input work and the head loss. Therefore, the head loss can be written as:

$$\psi_{loss} = (\psi_0 - \psi) - (\psi_{i0} - \psi_i) \tag{2}$$

Where the first parenthesis is the difference of apparent head rise decrement and the second parenthesis is the input work difference. Figure 13 shows the influence of β_{2B} on the head loss coefficient. It can be seen that the relative head loss coefficient diminishes with increasing β_{2B} for all tip clearances and flow rates. The influence of tip clearance ratios on the relative head loss coefficient is shown in Figure 14. The relative head loss coefficient initially rises rapidly as the tip clearance ratios increase and then flattens. The change of slope varies for different β_{2B} and decreases for smaller tip clearance ratios and higher β_{2B}. Also, the results indicate that the number of blades has little impact on the head loss induced by the tip clearance.

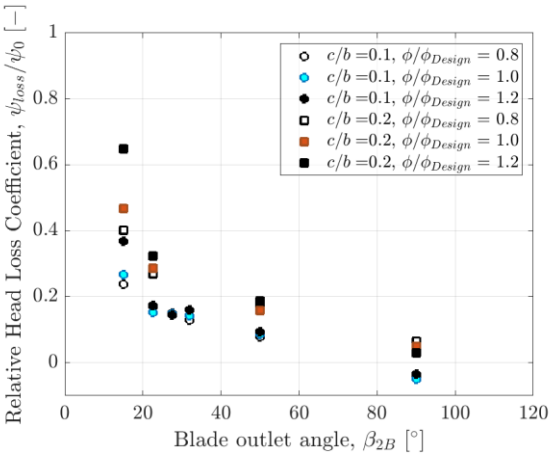

Figure 13 – Effect of blade outlet angle on relative head loss coefficient

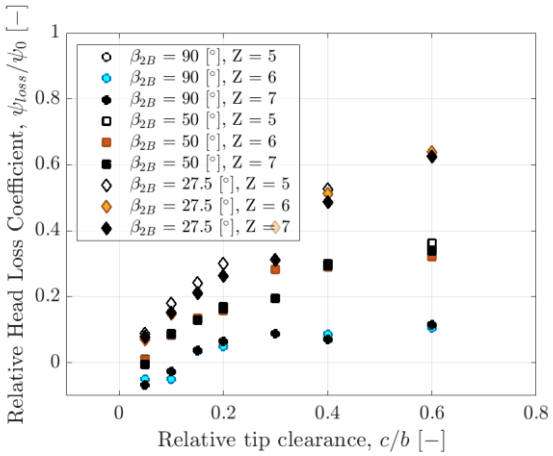

Figure 14 – Effect of tip clearance ratios on relative head loss coefficient

The reduced stagnation pressure (defined with Eq. (3) and Eq. (4)) is used to examine the loss distribution:

$$p_{T,r} = p_S + \frac{\rho}{2}(w^2 - u^2) \tag{3}$$

$$C_{p_{T,r}} = \frac{p_{T,r} - \overline{p_{T,r,inlet}}}{\rho u^2} \tag{4}$$

Figure 15 presents the non-dimensional stagnation pressure contour at the impeller outlet. With increasing tip clearance ratios, the minimum reduced stagnation pressure decreases, and the region with minimum values grows. This effect is more pronounced for lower β_{2B}. At larger tip clearance ratios, more flow leaks through the tip clearance and does not get completely mixed with the main flow. As a consequence, the reduced stagnation pressure decreases.

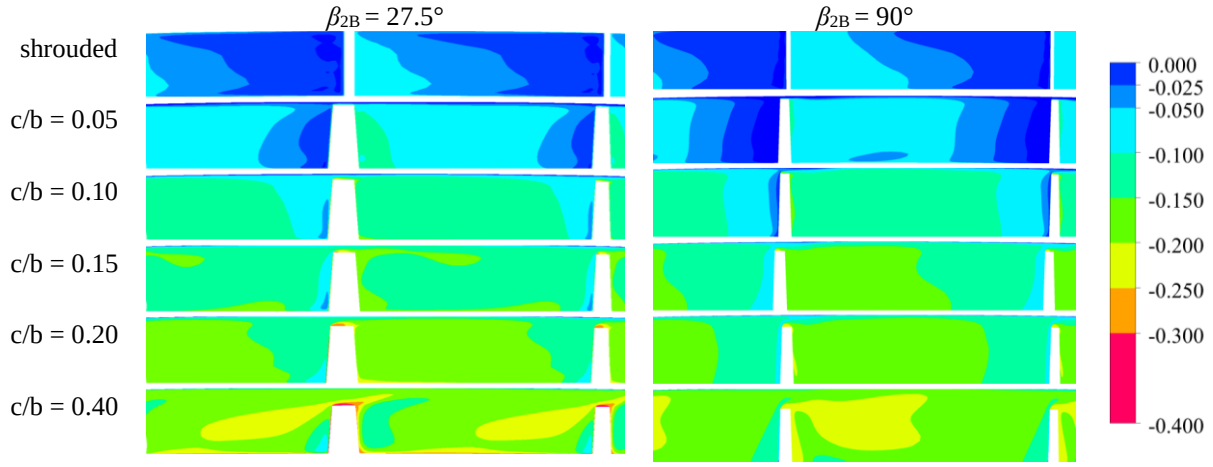

Figure 15 – Contours of non-dimensional reduced stagnation pressure contour ($C_{P_{T,r}}$) at the impeller outlet

3-3. Neural network model

To obtain more reliable prediction models for the slip and the head loss coefficient due to tip clearance, two neural network (NN) based surrogate models have been implemented. Although available models were correlated based on experimental data, the NN models of this study are trained on a much large number and a wider range of data points. The data used to train the slip factor model is obtained based on the parametric ranges listed in Table 1. 100 unshrouded impellers and their equivalent shrouded cases are randomly generated and solved with CFD, which then is used for testing the generated NN models. Test impellers do not share any common parameter with the training data and were randomly generated and used to evaluate the model. Hence, the test data is independent of the training data, except that both were evaluated using the same CFD setup.

The NN of this research is implemented using Flux (2018a) in the environment of Julia programming language. The core feature of Flux is the adoption of native Julia code to take gradients, which results in significantly lower computation time. The tip clearance ratio, β_{2B}, number of blades, β_{le}, the ratio of the inlet to outlet diameters, and the specific speed were taken as input parameters for the head loss coefficient model while the first three parameters and the flow coefficient were inputs of the slip factor model.

For the slip factor, the best algorithm is determined to be feedforward neural networks with two hidden layers of 5 neurons each with a sigmoid activation function. Figure 16 presents the relative deviation of slip factors predicted with the NN model for training and test data. The NN model predicts 100% of both training and test CFD data within a relative deviation of ±10%, yielding an average absolute deviation of 1.6% and 3.6% for training and test data respectively. Compared to 83% of data predicted within ±10% relative deviation by Von Backström (2006) correlation, the NN model improves the prediction accuracy of slip factors.

For the head loss coefficient, the optimized NN design consists of two hidden layers of 15 neurons each, with a sigmoid activation function. 100% of CFD data are predicted within a relative deviation of ±10%, as shown in Figure 17. Therefore, the NN models are capable of properly mapping arbitrary input data into their correct target values for the slip factor and head loss coefficient for small-scale turbopumps.

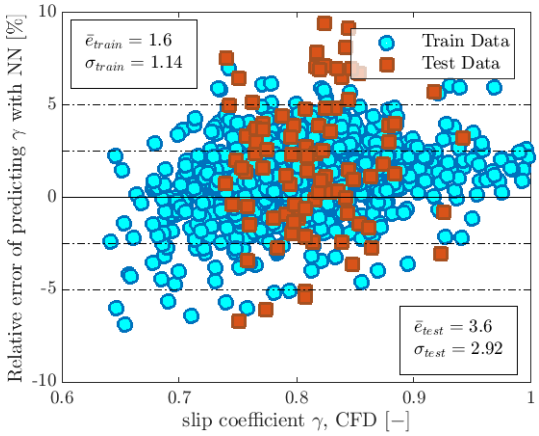

Figure 16 - Relative deviation of slip factor predicted with NN from CFD results

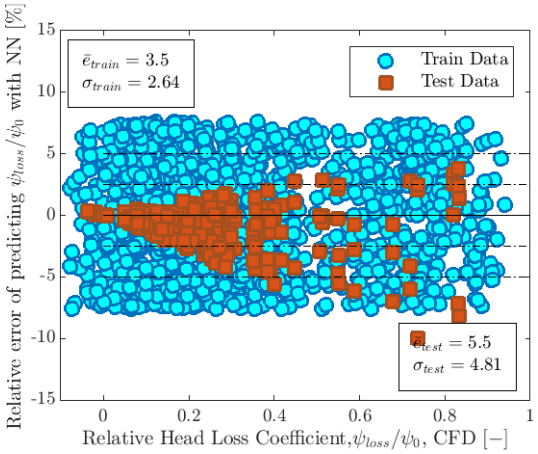

Figure 17 - Relative deviation of head loss coefficient predicted with NN from CFD results

CONCLUSIONS

A new robust design model was developed to generate 776 different impellers of small-scale turbopumps for ORC, covering a wide range of geometrical parameters. The influence of tip clearance, β_{2B}, number of blades, and flow rate on performance at design and off-design conditions are investigated and modeled. The key findings can be summarized as follows:

a) The tip clearance influences the slip factor non-linearly. At high β_{2B} (radial impellers), the effects of tip clearance and flow rate on the slip factor diminish.
b) The head rise decreases with tip clearance ratios. However, for radial impellers, a higher head rise was observed for small tip clearance ratios (<0.1). More investigation should be carried out to understand this observation.
c) The effect of tip clearance flow leads to complex flow patterns and a simple model cannot accurately consider the influential parameters affecting slip factor and performance of unshrouded impeller.
d) Neural networks were trained to model the influence of dominant parameters on the slip factor and head loss coefficient of unshrouded impellers. The models predicted the CFD data with the average relative deviation of 3.6 and 5.8 for the slip factor and the head loss coefficient, respectively. Thus, the models have successfully improved the performance prediction accuracy of centrifugal pumps.

NOMENCLATURE

b	blade height, m
c	clearance gap, m
c	absolute velocity, m s^{-1}
u	peripheral velocity, m s^{-1}
C_p	pressure coefficient
p_S	static pressure, Pa
$p_{T,r}$	reduced stagnation pressure, Pa
r	radius, m
Re	Reynolds number, $\rho u_2 r_2/\mu$
w	relative velocity, m s^{-1}
Z	number of blades
Greek letters	
β	flow angle, °
β_B	blade angle, °
ρ	density, kg m^{-3}
μ	viscosity, Pa s
γ	slip factor
Φ	flow coefficient
ψ	head coefficient
n_q	specific speed (rpm, m^3, m)
Subscripts	
i	input
u	circumferential component
m	meridional component
2	outlet station
0	shrouded impeller
Abbreviations	
CFD	computational fluid dynamics
ORC	organic Rankine cycle
NN	neural network

REFERENCES

Aknouche, Sebasien. 2003a. “Impact of Tip Clearance Flow on Centrifugal Pump Impeller Performance by Sebastien Aknouche.” Massachusetts Institute of Technology. dspace.mit.edu/handle/1721.1/82254.

von Backström, Theodor. 2006. “A Unified Correlation for Slip Factor in Centrifugal Impellers.” *Journal of*

Turbomachinery-transactions of The Asme - J TURBOMACH-T ASME 128.

Busemann, As. 1928. "Das Förderhöhenverhältnis Radialer Kreiselpumpen Mit Logarithmisch-Spiraligen Schaufeln." *ZAMM-Journal of Applied Mathematics and Mechanics/Zeitschrift für Angewandte Mathematik und Mechanik* 8(5): 372–84.

Diehl, Markus, Christoph Schreiber, and Jürg Schiffmann. 2020. "The Role of Reynolds Number Effect and Tip Leakage in Compressor Geometry Scaling at Low Turbulent Reynolds Numbers." *Journal of Turbomachinery* 142(3). http://infoscience.epfl.ch/record/276559.

Eck, Bruno. 1973a. "Fans." *1st English ed., Pergamon Press, Oxford*: 139–53.

Eum, Hark Jin, Young Seok Kang, and Shin Hyoung Kang. 2004. "Tip Clearance Effect on Through-Flow and Performance of a Centrifugal Compressor." *KSME International Journal* 18(6): 979–89.

Gülich, JF. 2010. *Centrifugal Pumps*. Berlin, Heidelberg: Springer. https://link.springer.com/content/pdf/10.1007/978-3-540-73695-0.pdf (July 1, 2019).

Innes, Mike. 2018a. "Flux: Elegant Machine Learning with Julia." *Journal of Open Source Software*.

Ishida, Masahiro, Yasutoshi Senoo, and Hironobu Ueki. 1989. "Secondary Flow Due to the Tip Clearance at the Exit of Centrifugal Impellers." *Proceedings of the ASME Turbo Expo* 1(January): 19–24.

Lu, Yeming, Xiaofang Wang, and Rong Xie. 2017. "Derivation of the Mathematical Approach to the Radial Pump's Meridional Channel Design Based on the Controlment of the Medial Axis." *Mathematical Problems in Engineering* 2017: 1–15.

Menter, Florian, M Kuntz, and R B Langtry. 2003b. "Ten Years of Industrial Experience with the SST Turbulence Model." *Heat and Mass Transfer* 4.

Pampreen, R. C. 1973b. "Small Turbomachinery Compressor and Fan Aerodynamics." *Journal of Engineering for Gas Turbines and Power* 95(3): 251–56.

Rosset, Kévin, Violette Mounier, Eliott Guenat, and Jürg Schiffmann. 2018b. "Multi-Objective Optimization of Turbo-ORC Systems for Waste Heat Recovery on Passenger Car Engines." *Energy*.

Rosset, Kévin, Olivier Pajot, and Jürg Schiffmann. 2021. "Experimental Investigation of a Small-Scale Organic Rankine Cycle Turbo-Generator Supported on Gas-Lubricated Bearings." *Journal of Engineering for Gas Turbines and Power* 143(5): 1-14,51015. http://infoscience.epfl.ch/record/285103.

Senoo, Y., and M. Ishida. 1984. "Pressure Loss Due to the Tip-Clearance of Impeller Blades in Centrifugal and Axial Blowers." 108((Lecture Ser. 1984-07)).

Stanitz, J D. 1952. "Some Theoretical Aerodynamic Investigations of Impellers in Radial and Mixed Flow Centrifugal Compressors." *Trans. ASME* 74(4): 473–97.

Stepanoff, AJ. 1957. *Centrifugal and Axial Flow Pumps : Theory, Design, and Application*. New York: Wiley.

Stodola, Aurel. 1927. 2 *Steam and Gas Turbines: With a Supplement on the Prospects of the Thermal Prime Mover*. McGraw-Hill.

Wiesner, F. J. 1967. "A Review of Slip Factors for Centrifugal Impellers." *Journal of Engineering for Gas Turbines and Power*.

Wood, G. M., H. Welna, and R. P. Lamers. 1965. "Tip-Clearance Effects in Centrifugal Pumps." *Journal of Fluids Engineering, Transactions of the ASME* 87(4): 932–39.

Zou, Jun, Pengfei Wang, Xiaodong Ruan, and Xin Fu. 2012. "A Statistical Method on Meridional Profiles of Centrifugal Pumps." *Journal of Fluids Engineering* 134(2): 024502.